frontiers | Frontiers in Earth Science

TYPE Original Research
PUBLISHED 13 August 2024
DOI 10.3389/feart.2024.1448238

OPEN ACCESS

EDITED BY
Hu Li,
Sichuan University of Science & Engineering, China

REVIEWED BY
Guoping Liu,
Peking University, China
Hongsheng Wang,
The University of Texas at Austin, United States

*CORRESPONDENCE
Lei Gong,
kcgonglei@foxmail.com
Shuai Gao,
349684871@qq.com

RECEIVED 13 June 2024
ACCEPTED 29 July 2024
PUBLISHED 13 August 2024

CITATION
Wang J, Wang J, Zhang Y, Zhang D, Sun L, Luo J, Wang W, Gong L, Liu Z and Gao S (2024) Multi-scale fracture patterns and their effects on gas enrichment in tight sandstones: a case study of the Upper Paleozoic in the Qingshimao gas field, Ordos Basin, China. *Front. Earth Sci.* 12:1448238. doi: 10.3389/feart.2024.1448238

Multi-scale fracture patterns and their effects on gas enrichment in tight sandstones: a case study of the Upper Paleozoic in the Qingshimao gas field, Ordos Basin, China

Jie Wang[1], Jiping Wang[2,3], Yuanyuan Zhang[2,3], Daofeng Zhang[2,3], Lei Sun[2,3], Jianning Luo[2,3], Wei Wang[2,3], Lei Gong[1,4]*, Zongbao Liu[1] and Shuai Gao[1,4]*

[1]College of Geosciences, Northeast Petroleum University, Daqing, China, [2]Exploration and Development Research Institute of China Petroleum Changqing Oilfield Company, Xi'an, China, [3]National Engineering Laboratory for Exploration and Development of Low Permeability Oil and Gas Fields, Xi'an, China, [4]Bohai-Rim Energy Research Institute, Northeast Petroleum University, Qinhuangdao, China

A well-connected network formed by multi-scale fractures is a key factor in the formation of high-quality reservoirs and the achievement of high and stable oil and gas production in tight sandstones. Taking the Upper Paleozoic of the Qingshimao gas field in the Ordos Basin, China, as an example, based on data from image logs, cores, and thin sections, fine quantitative characterization of multi-scale natural fractures in tight sandstone reservoirs was carried out. We also established a method for dividing network patterns of multi-scale fractures and discussed the effect of each fracture network pattern on the gas enrichment and production capacity. Results indicate regular changes in the length, density, aperture, porosity, permeability, and connectivity of natural fractures at different scales. Based on the spatial combination patterns and connectivity of fractures of different scales, four types of fracture network patterns were established: multi-scale fracture network with high density and multi-orientations, multi-scale fracture network with moderate-high density and dual orientations, small-scale fracture network with moderate density and dual orientations, small-scale fracture network with low density and single orientation. The first fracture network pattern can destroy the integrity of the cap layer, causing natural gas leakage. The second fracture network pattern is a favorable area for natural gas enrichment. The third fracture network pattern requires the use of hydraulic fracturing to obtain commercial airflow. The fourth fracture network pattern has little effect on reservoir control and storage. The study of natural fractures in tight sandstone reservoirs is usually based on a single-scale perspective. Understanding the development characteristics of multi-scale fractures and their controlling effects on the reservoir helps to

comprehensively understand the spatial configuration relationship of multi-scale fracture network structure patterns and promotes the development of multi-scale fractures in tight reservoir research.

KEYWORDS

Qingshimao gas field, tight sandstone, multi-scale fractures, fracture network pattern, gas enrichment

1 Introduction

Tight sandstone gas has become one of the essential fields for global unconventional natural gas exploration and development (Farouk et al., 2024). According to statistics from the Federal Geological Survey of the United States, approximately 70 tight gas basins have been discovered or speculated to develop globally, with tight gas resources of approximately 310 × 10^{12}m^3-510 × 10^{12}m^3 (German et al., 2023; Jia et al., 2012). As of the end of 2023, the cumulative proven reserves of the Upper Paleozoic in the Qingshimao area were 1,459 × 10^8 m^3, demonstrating good exploration prospects (He et al., 2021). The preliminary exploration results have confirmed that natural fractures are the key factor for obtaining high gas flow in the tight sandstone reservoir (Balsamo et al., 2023; Vásquez Serrano et al., 2024).

Natural fractures are not only effective storage spaces for tight sandstone reservoirs, but also essential seepage channels (Ortega et al., 2006; Gale et al., 2007; Gale et al., 2014; Gong et al., 2021b; Gong et al., 2023a; Zeng et al., 2024). Numerous studies by scholars have shown that the development of natural fractures exhibits multi-scale distribution characteristics (Guerriero et al., 2011; Micheal et al., 2021; Sweeney M R, 2023). They can quantitatively characterize fracture parameters at different scales based on observation methods or data such as nano CT, scanning electron microscopy, microscopic thin sections, core observation, logging interpretation, field outcrops, and drone photography (Loza Espejel et al., 2020; Birkholzer et al., 2021). The parameter characterization of fractures of different scales can span multiple orders of magnitude, and scholars have also studied different scales of fractures based on their own research purposes (Ortega et al., 2006; Strijker et al., 2012). The multi-scale natural fracture system not only communicates various pores and enhances the reservoir's permeability, but also is a key factor affecting the high production of tight sandstone reservoirs (Gong L. et al., 2019; Birkholzer et al., 2021; Nwabia and Leung, 2021; Sweeney et al., 2023). Fractures of different scales have different lengths and openings, resulting in varying degrees of connectivity and significant differences in their contributions to tight sandstone reservoirs (Bertrand et al., 2015; Laubach et al., 2018; Prabhakaran et al., 2021). The configuration combination and spatial distribution pattern of fractures of different scales are the key to determining whether an effective continuous reservoir can be formed (Fu J. H. et al., 2022; Fu X. F. et al., 2022; Sweeney M R, 2023). The degree of development, porosity, and permeability of fractures at different scales vary to some extent, but they have a positive effect on productivity (Watkins et al., 2018; Aubert et al., 2021; Cao et al., 2024). In other words, there is a positive correlation between the development degree of the multi-scale natural fractures and production capacity. The higher the development degree of the multi-scale natural fractures, the higher the production capacity of the oil and gas wells (Bagni et al., 2020; Fu et al., 2023; Zeng et al., 2023).

However, with the deepening of exploration and development of tight sandstone gas reservoirs, the contradiction between the fracture development degree and natural gas production capacity has become increasingly prominent, that is, there may not necessarily be a positive correlation between the fracture intensity and production capacity (Gong Lei. et al., 2019). Part of the reason for this contradiction is that there are scale differences in the sources of obtaining fracture strength data, resulting in poor comparability of fracture strength across different wells. At the same time, the differences in connectivity and contribution to reservoir properties of fractures of different scales were also ignored, exposing the problem of unclear understanding of the development characteristics and spatial configuration patterns of multi-scale fractures in tight sandstone reservoirs (Zeng et al., 2022). The fracture development degree is not the only factor determining the high and stable production of a single well. Previous studies on multi-scale fractures have been limited, and currently only targeted research has been conducted on fractures of a certain scale, lacking evaluation of the development characteristics of fractures at multiple scales. (Watkins et al., 2015; Casini et al., 2016; Fernández-Ibáñez et al., 2018; Prabhakaran et al., 2021). Meanwhile, the role of multi-scale fracture development characteristics in reservoir control and storage also needs to be studied. As a typical tight sandstone gas development area in China, the Qingshi Mao gas field also faces such problems.

Therefore, taking the Upper Paleozoic tight sandstone reservoir of the Qingshimao gas field in Ordos Basin as an example, we quantitatively characterized the genesis types and distribution characteristics of multi-scale fractures, clarified the distribution mode of multi-scale fractures and their contributions to the reservoir, established the fracture network pattern of the Qingshimao gas field, and discussed the fracture development characteristics of each fracture network pattern and their controlling effect on gas accumulation.

2 Geological setting

The Qingshimao gas field is located in the western part of the Ordos Basin in China (Figure 1A). Structurally, it is situated on the southern wing of the central uplift of the Tianhuan Depression in the Ordos Basin and is in contact with the Majiatan Fault on the west side (Figure 1B). The Majiatan Fault is mainly characterized by a Y-shaped reverse thrust and detachment, exhibiting an overall SN-oriented asymmetric syncline shape with obvious north-south segmentation and east-west zoning (Guo et al., 2020). The

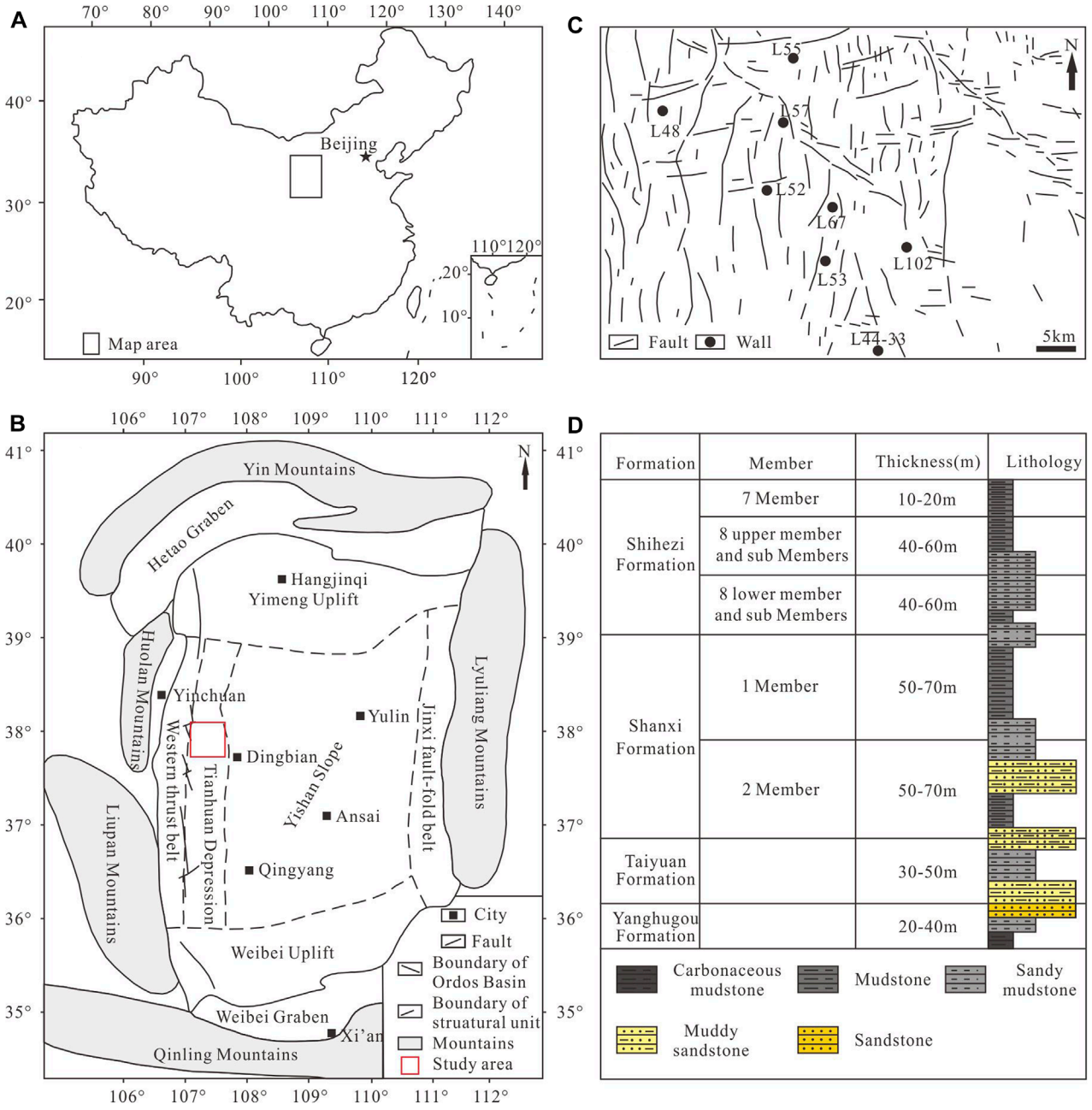

FIGURE 1
Location, structural outline, and stratigraphic overview of the Qingshimao gas field. **(A)** The location of the Ordos Basin. **(B)** The location of the Qingshimao gas field. **(C)** Overview of the Structure of Qingshimao Gas Field **(D)** Overview of the Strata of Qingshimao Gas Field.

overall structural morphology of the research area is high in the north and low in the south, with a northwest-southeast trending nose-shaped uplift. Three northwest southeast trending faults are developed on the nose uplift belt, and nearly north-south trending secondary faults are developed in the south and east (Yin et al., 2022) (Figure 1C).

The strata in the Qingshimao area are tight sandstone reservoirs, with the Carboniferous Benxi Formation, Permian Taiyuan Formation, Shanxi Formation, Lower Shihezi Formation, Upper Shihezi Formation, and Shiqianfeng Formation developed from bottom to top (Figure 1D). The internal sedimentation is continuous, all of which are integrated contacts, mainly composed of transitional facies between sea and land and inland lake basin sedimentation. The main gas-bearing intervals are the He 8 section of the Permian Shihezi Formation, the Shan 1 and Shan 2 sections of the Shanxi Formation, and the Taiyuan Formation. The thickness of the Upper Paleozoic strata is relatively stable in this area, with a total sedimentary rock thickness of about 700 m and minimal planar variation (Jiang et al., 2023). Its lithology is mainly composed of tight sandstone, with the main rock types being siltstone, fine sandstone,

quartz sandstone, and interbedded mud and sand. The Taiyuan and Shanxi formations of the Permian are mainly sedimentary coal-bearing strata, the main source rocks of the Upper Paleozoic. The physical properties of the reservoir in the typical well of tight sandstone in the Qingshimao gas field are different, with porosity distribution ranging from 5% to 11%, with an average of 7.9%. The permeability distribution is between 0.1 and 4.2mD, with an average of 0.36mD. The differences in the physical properties of sandstone reservoirs may be related to the quartz content and cement types in different regions, with higher quartz content areas having better reservoir properties (Wang et al., 2022; Su et al., 2023).

3 Method

3.1 Materials and samples

We use image logs data from 36 wells to identify natural fractures and quantitatively characterize parameters such as fracture occurrence (strikes and dip angles), density, and aperture. We observed and described 210 m core samples from 5 wells in the Qingshimao gas field (Figure 1C). We measured parameters such as the type, mechanical properties, dip angle, height, aperture, and filling degree of 1,320 fractures. At the same time, we selected characteristic wells from the distance of the fault and integrated their gas and water production data to analyze the reservoir control effect in the study area. The Zeiss Axio Image Z1 polarizing microscope was used to statistically analyze the fracture parameters (fracture type, filling degree, aperture, length) of 40 cast thin sections. According to the method proposed by Zeng et al. (2010), the aperture of fractures under formation-confining pressure conditions was corrected, and the porosity and permeability of fractures of different scales were calculated using the Monte Carlo method.

3.2 Characterization of fracture connectivity

Sanderson et al. (2018) proposed a topological representation method for fracture network patterns, which provides convenience for characterizing fracture connectivity. They divided the types of fracture nodes into isolated nodes (Type I), adjacent nodes (Type Y), and intersecting nodes (Type X), indicating that the degree of fracture connectivity has gradually improved. At the same time, they used the ratio of the number of branches to the number of fractures (NB/NL) and the number of nodes occupied by each fracture (CL) to characterize the connectivity of fractures (Balberg and Binenbaum, 1983; Berkowitz, 1995; Manzocchi, 2002; Sanderson and Nixon, 2015). A large number of real fracture network pattern statistics and numerical simulations confirm that the NB/NL values are distributed between 2–10, and the larger the NB/NL value, the better the connectivity. When CL < 2, it indicates that the fracture network is not connected. When CL > 3.57, the fracture network reaches a percolation state (Balberg et al., 1984; Nixon et al., 2012). Attila Petrik et al. (2023) improved and optimized the characterization of fracture connectivity based on the Sanderson topology using high-resolution image logs technology (Petrik et al., 2023). However, this method must be based on a definite fracture network graph. Since our study area can directly observe very few intersecting fractures on core and image logs, it is difficult to observe adjacent nodes (Y-shaped nodes) and intersecting nodes (X-shaped nodes). It is difficult for us to directly use Sanderson and Attila Petrik's methods to quantitatively characterize the connectivity of fractures in the study area. Ghosh and Mitra. (2009) and Gong et al., 2023a studied the factors affecting fracture connectivity and pointed out that fracture density, fracture orientation and sets, and fracture length are the main factors affecting fracture connectivity (Ghosh and Mitra, 2009; Gong et al., 2023a). We are inspired by this and propose a fracture connectivity prediction method based on considering these influencing factors. Firstly, the Monte Carlo random simulation method is used to create a fracture pattern with the actual fracture density, sets and orientation, fracture length, and other parameters in the study area as constraints. Then, Sanderson's method is used for connectivity characterization. The connectivity of the fractures in the study area can be equivalently calculated through dozens of simulations and characterisations.

4 Results

Based on the identification methods and scale of natural fractures, as well as the arrangement relationship between fractures and mechanical layers, natural fractures in tight sandstone in the study area can be divided into three types: large-scale fractures, small-scale fractures and micro-scale fractures. Large-scale fractures are manifested as throughgoing fractures and small faults, which generally cut through multiple rock mechanical units. Some small faults can cut through mudstone interbeds or throughgoings. Small-scale fractures are mainly manifested as bed-confined fractures (including intraformational fractures), which develop within a single rock mechanical layer and are mainly controlled by beddings and lithological interfaces. Micro-scale fractures are smaller in scale, generally less than 50 μm in aperture, and can only be identified under microscope.

4.1 Large-scale fractures

Three types of fractures, conductive, resistive and induced, were identified on image logs. Conductive fractures are characterized by dark sinusoidal curves, generally open fractures that are not filled with minerals. Resistive fractures are characterized by bright sinusoidal curves, typically natural fractures filled with calcite or quartz (Figures 2A,B). Induced fractures are usually caused by drilling tool disturbance or stress release, indicating the direction of the current maximum principal stress at present and thus indirectly used to evaluate the effectiveness of the fracture. Large-scale fractures exhibit dark (or bright) sinusoidal curves at medium to high dip-angles in image logs and have continuous and good penetrability (Figures 3A,B), with some showing apparent bedding plane displacement or small displacement on both sides of the fracture surface. On the core, it exhibits high dip-angle throughgoing fractures that cut through multiple rock mechanical layers (interfaces) (Figures 3C,D).

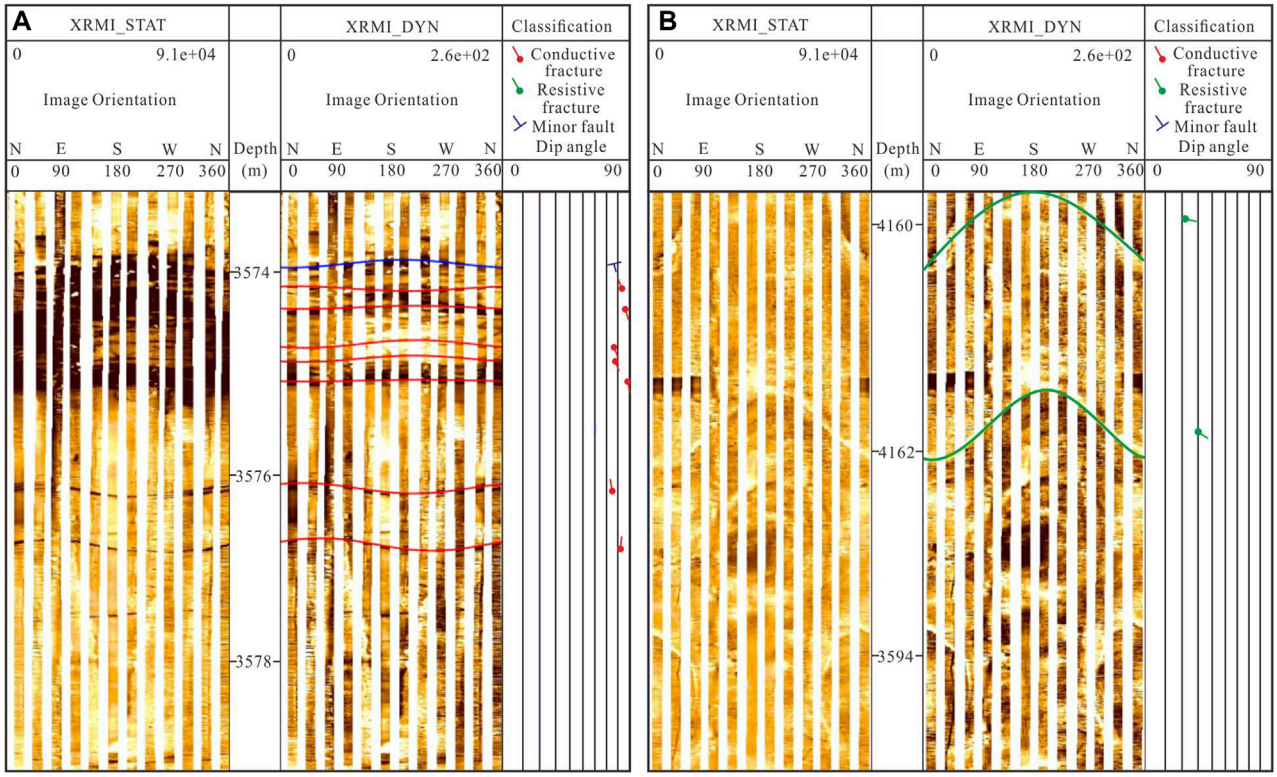

FIGURE 2
Types of image logs fractures in the study area. **(A)** The characteristics of high conductivity fractures and small faults were identified by image logs. **(B)** High resistance fracture characteristics identified by image logs.

The tight sandstone reservoir in the Qingshimao gas field mainly develops four sets of fractures: northeast-southwest, northwest-southeast, nearly north-south, and nearly east-west. Most of the wells mainly comprise two sets of fractures: northeast-southwest and nearly north-south. Some wells exhibit a single orientation, but the wells near the fault are greatly affected by the structure. The fracture orientation is relatively complex, with three to four sets of fractures developed. The inclination angle of large-scale fractures is mainly medium to high dip-angle, mainly distributed at 60°–90°, accounting for more than 85%, while a small number of low dip-angle fractures are developed (Figure 4). High conductivity fractures account for about 92% of the image logs fractures in large-scale fractures, and their effectiveness is good. Consistent with the observation results of the core. The density of fracture lines is distributed between 0.3–0.6 lines/m, with an average of 0.47 lines/m, and there are differences in fracture density among different wells. The aperture of large-scale fractures is mainly distributed between 55–180° μm. The average is 108 μm. According to the Monte Carlo method, the porosity and permeability of fractures were calculated, and it was found that the porosity of large-scale fractures is relatively low, mainly distributed in the range of 0.07%–0.15%, with an average of 0.10%. Its permeability is relatively high, with a main distribution range of 8-10mD and an average of 9.2mD.

A planar fracture connectivity network model was established based on the constraints of the fracture group and orientation, fracture scale, and fracture density mentioned above. Sanderson's fracture connectivity characterization method is used to characterize natural fractures in the tight sandstone reservoir of the Qingshimao gas field under this mode. Twenty simulations were conducted on large-scale fractures, and the simulation results showed that the proportion of isolated type nodes (Type I nodes) in the study area ranged from 34.6% to 47.2%, with an average of 40.9%; The proportion of adjacent nodes (Y-shaped nodes) is distributed between 3.5% and 18.4%, with an average of 10.3%; The proportion of intersecting nodes (X-shaped nodes) is distributed between 45.6% and 54.4%, with an average of 48.6%. The number of nodes (CL) for each fracture is mainly distributed between 3.35–5.84, with an average of 5.18, and the majority of them are greater than 3.27. In the IYX triangle diagram, the simulation results are generally located in the fracture seepage zone, with a small portion located in the critical seepage zone.

4.2 Small-scale fractures

Small-scale fractures in tight sandstone reservoirs in the Qingshimao area are manifested on the core as intraformational fractures developed within the rock mechanics layer and bed-confined fractures terminated at the rock mechanics interface at the end. The intraformational fractures within the layer are characterized by no contact between the two ends and the interface of the rock mechanics layer. The fracture size is small, the height is smaller than the thickness of the developed rock mechanics

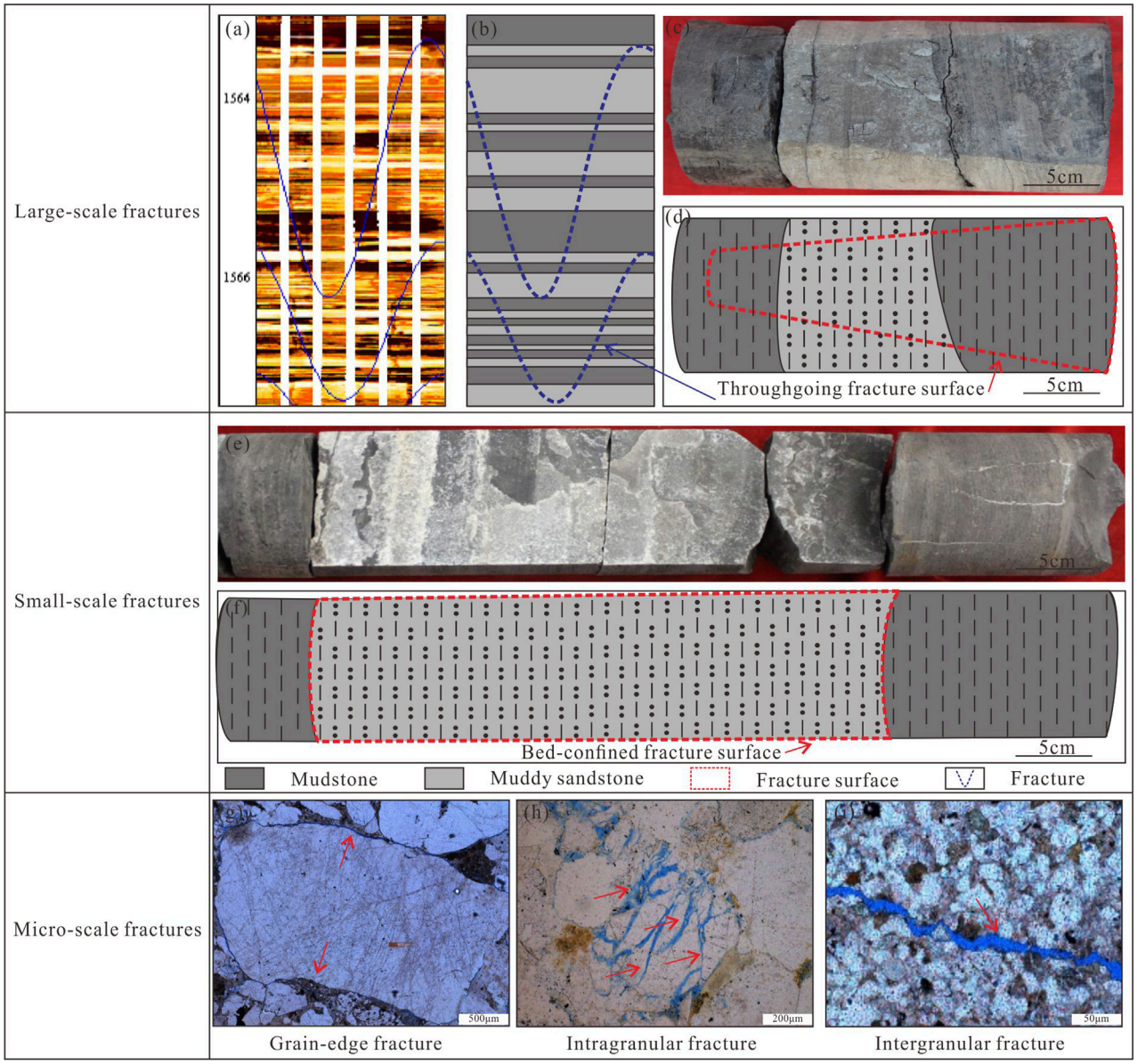

FIGURE 3
Characteristics of multi-scale fractures. **(A)** and **(B)** Throughgoing fractures in image logs; **(C)** and **(D)** Throughgoing fractures in cores; **(E)** and **(F)** Bed-confined fractures in cores; **(G)** Grain-edge fractures in thin section; **(H)** Intragranular fractures in thin section; **(I)** Intergranular fractures in thin section.

layer, and the fracture aperture is smaller. Bed-confined fractures are limited by the interface between the rock mechanics layers on both sides, with one or both ends terminating at the rock mechanics layer interface. The fracture height is less than or equal to the thickness of the developed rock mechanics layer, the fracture surface is rough, the aperture is greater than the aperture of the intraformational fracture, the fracture inclination is large, and it is distributed nearly perpendicular to the rock mechanics interface. The fracture distribution is regular, and the spacing is good (Figures 2E,F).

The inclination angle of small-scale fractures in the tight sandstone reservoir of the Qingshimao gas field is mainly high dip-angle, mainly distributed at 80°–90°. The height of fractures is mainly distributed between 5 and 25cm, with an average of 19.2 cm. The filling degree of small-scale fractures is very low, with 10.47% fully filled, 1.16% partially filled, 88.37% unfilled, and 89.53% effective fractures. The effectiveness of fractures is good, and the filling minerals are mainly calcite, quartz, and mud (Figure 5). The linear density of small-scale fractures is mainly distributed between 0.52–2.07/m, with an average of 1.04/m. The degree of fracture development varies among different wells and regions. The aperture of small-scale fractures is mainly distributed between 80–100° μm. The average is 85 μm. The porosity of fractures is mainly distributed between 0.17% and 0.23%, with an average of 0.20%. The permeability of fractures is mainly distributed between 2-8mD, with an average of 3.6mD.

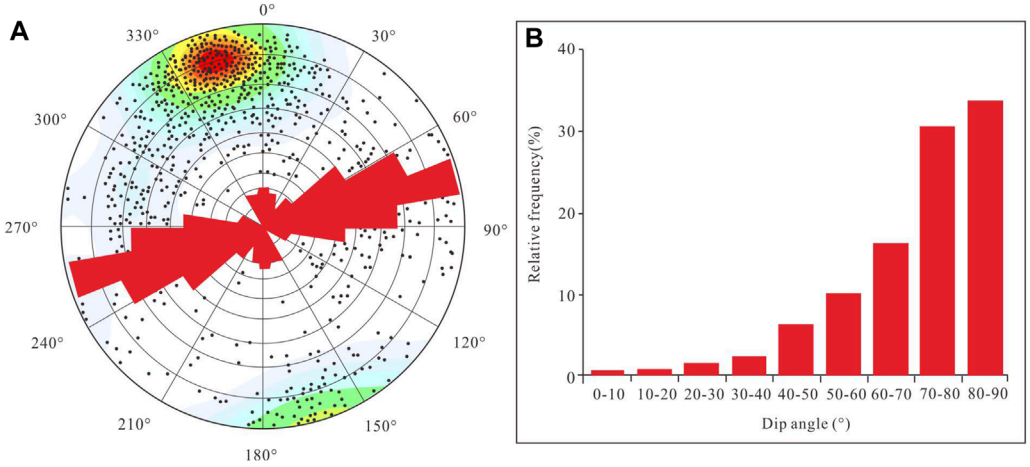

FIGURE 4
Rose plot and dip distribution of natural fractures in the study area. **(A)** Rose diagram of natural fracture direction. **(B)** Distribution map of natural fracture inclination angle.

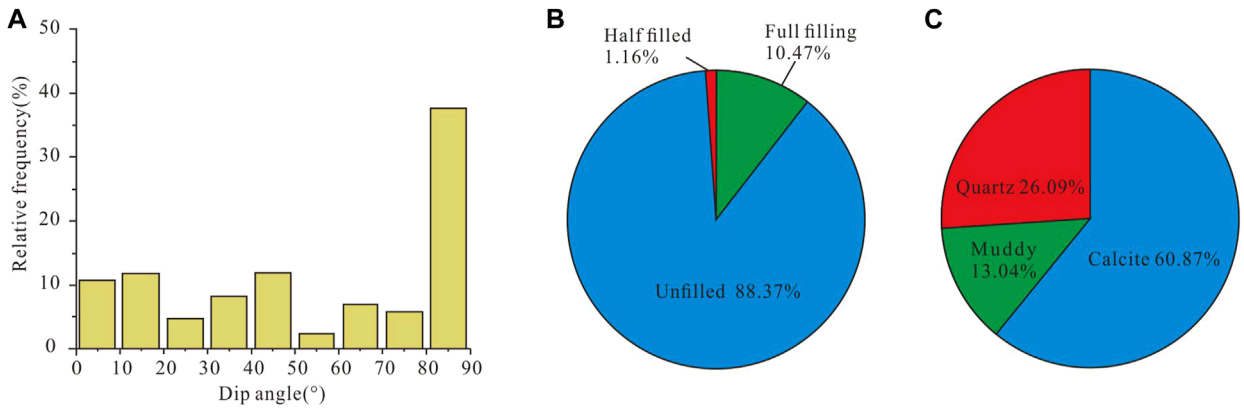

FIGURE 5
Various parameters of small-scale fractures. **(A)** Distribution map of dip angle of bed-confined fractures. **(B)** Distribution map of fracture filling degree. **(C)** Fill with minerals.

Due to the core's unoriented nature, we cannot obtain the orientation information of small-scale fractures. Since the study area is mainly composed of structural fractures, small-scale and large-scale fractures have the same composition and orientation. Therefore, we used the composition and orientation of large-scale fractures determined by image logs and the density, scale, and composition of small-scale fractures on the core to constrain their connectivity and conducted 20 simulations of their fracture connectivity. The simulation results show that the proportion of isolated small-scale fracture nodes (Type I nodes) in the study area is distributed between 47.5%–60.1%, with an average of 53.6%; The proportion of adjacent nodes (Y-shaped nodes) is distributed between 4.2% and 19.3%, with an average of 12.5%; The proportion of intersecting nodes (X-shaped nodes) is distributed between 31.8% and 45.6%, with an average of 33.9%. The number of nodes (Cl) for each fracture ranges from 2.85 to 3.74, with an average of 3.22. In the IYX triangle diagram, the simulation results are generally located in the critical seepage area of the fracture, with a small portion located in the seepage area of the fracture (Figure 6).

4.3 Micro-scale fractures

According to the particle relationship between micro-fractures and minerals, they can be divided into intragranular fractures, grain edge fractures, and intergranular fractures (Figures 2G–I). According to the observation and statistics of micro-fractures in 40 casting thin sections, the micro-fractures in the Qingshimao gas field are mainly manifested as intergranular fractures on the thin sections and its content accounts for about 90%, with a relatively small proportion of intragranular fractures and grain-edge fractures and the content of both accounts for about 10%. The intergranular fracture usually cuts through multiple mineral particles, with a large aperture and long extension, partially penetrating the entire

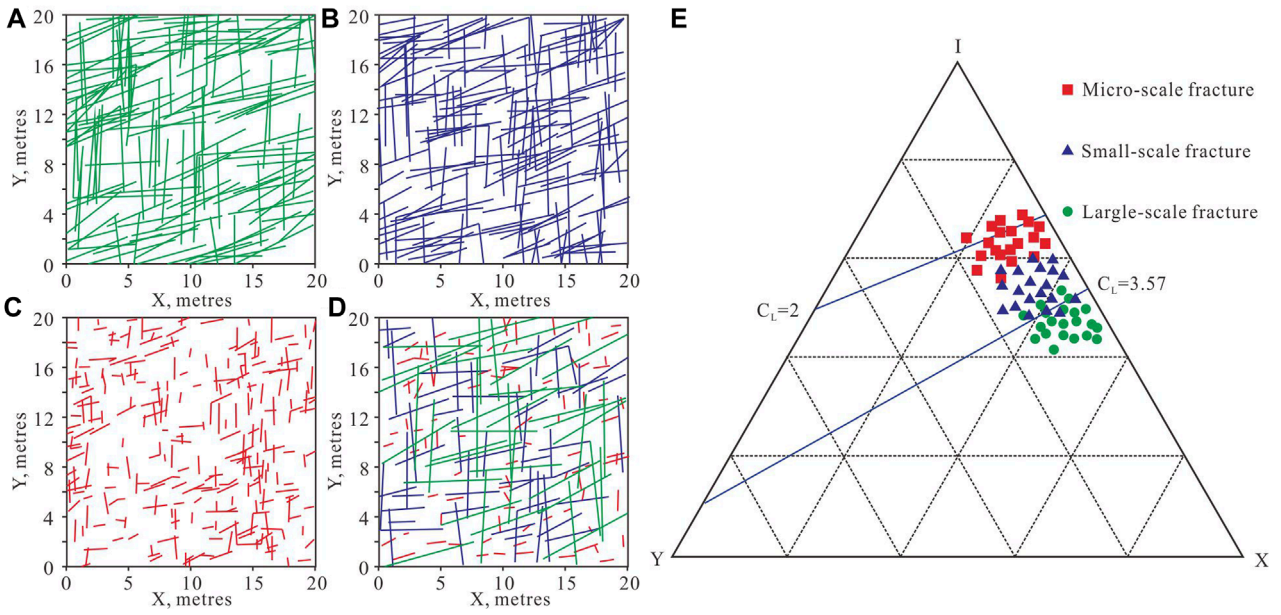

FIGURE 6
Characterization of fracture connectivity at different scales. **(A)** Simulation of multi-scale fracture connectivity. **(B)** Large-scale fracture connectivity simulation **(C)** Small-scale fracture connectivity simulation **(D)** Micro-scale fracture connectivity simulation **(E)** Multi-scale fracture connectivity triangle diagram.

thin film development, mainly playing a role in communicating the pores between particles and within particles. Intragranular fractures are manifested as quartz fractures or feldspar cleavage fractures, usually distributed inside mineral particles without cutting through the edges of the particles, and their aperture is relatively small; The grain-edge fractures are distributed along the edges of mineral particles, with a smaller aperture.

The filling degree of micro-scale fractures in the tight sandstone reservoir of the Qingshimao gas field is relatively low, with full filling accounting for 16%, semi-filling accounting for 32%, unfilled accounting for 52%, and effective fractures accounting for 84%. The effectiveness of fractures is good, and the minerals used for fracture filling are calcite, quartz, and mud. The development degree of micro-scale fractures is high, and the density of fracture surfaces is mainly distributed between 1 and 6.8 m/m^2, with an average of 4.2 m/m^2. The aperture of micro-fractures is mainly distributed between 10 and 75 μm. Its peak value is 128 μm. The average is 48.6 μm. The aperture of unfilled fractures is mainly distributed between 8–145° μm. Its peak value is 143 μm. The average is 42.2 μm. The porosity of micro-fractures is mainly distributed between 0.1% –0.6%, with an average of 0.48%. The permeability of micro-fractures is mainly distributed between 0.01 and 0.1mD, with an average of 0.08mD (Figure 7).

Due to the core's unoriented nature, we cannot obtain information on the orientation of micro-scale fractures. Since that the study area is mainly composed of structural fractures, micro-scale and large-scale fractures have the same composition and orientation. Therefore, we used the composition and orientation of small-scale and large-scale fractures determined by image logs and the length, density, and composition of micro-scale fractures on thin sections, to constrain their connectivity, and conducted 20 simulations. The simulation results show that the proportion of isolated micro-scale fracture nodes (Type I nodes) in the study area is distributed between 55.6%–68.2%, with an average of 62.8%; The proportion of adjacent nodes (Y-shaped nodes) is distributed between 3.2% and 19.6%, with an average of 12.8%; The proportion of intersecting nodes (X-shaped nodes) is distributed between 19.2% and 35.6%, with an average of 24.4%. The number of nodes (CL) for each fracture ranges from 1.82 to 3.06, with an average of 2.52. In the IYX triangle diagram, the simulation results are generally located in the critical seepage area of the fracture, with a small portion located in the area of poor fracture connection and poor fracture connectivity (Figure 6).

5 Discussion

5.1 The control effect of multi-scale fractures on reservoirs

Scholars have found through reports on the characterization of fractures at different scales that there are regular variations in fracture parameters, such as fracture size, fracture effectiveness, fracture density, fracture aperture, porosity, permeability, and connectivity (Ortega et al., 2006; Guerriero et al., 2010; Guerriero et al., 2011; Strijker et al., 2012; Ghanizadeh et al., 2015). From micro-scale to small-scale to large-scale fractures, their fracture apertures are significantly different, showing an overall upward trend, distributed between 10–180° μm. However, the density and size of fractures at different scales exhibit opposite patterns. There are certain differences in the effectiveness of fractures of different scales, but this difference seems to have a

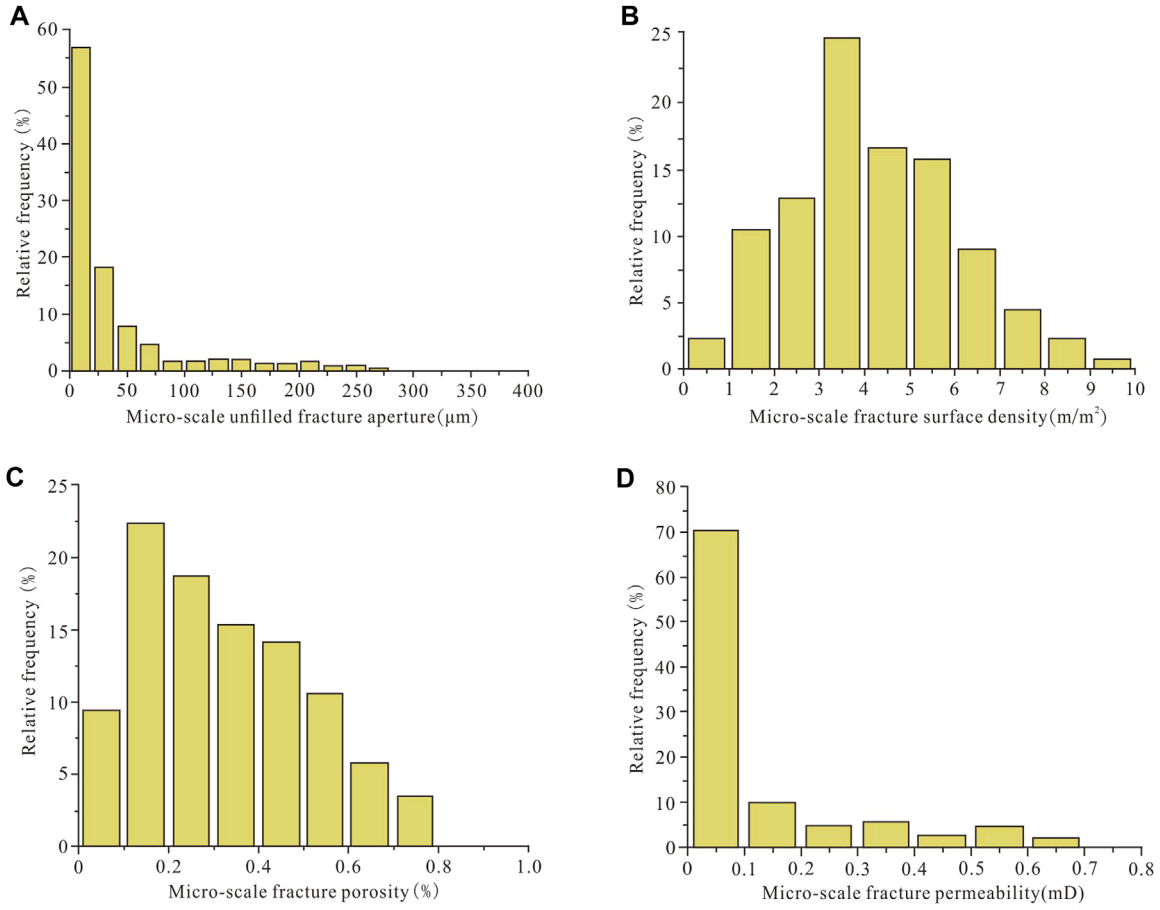

FIGURE 7
Distribution of various parameters of micro-scale fractures. **(A)** Distribution of micro-scale unfilled fracture aperture. **(B)** Distribution of micro-scale surface fracture density. **(C)** Distribution of micro-scale fracture porosity. **(D)** Permeability distribution of micro-scale fractures.

certain pattern: Micro-scale fractures have the worst effectiveness, while large-scale fractures have the best effectiveness. The reason for this difference may be that, from a microscopic perspective, the aperture of micro-scale fractures is smaller and more easily filled by minerals. On the other hand, from a macro perspective, some large-scale filled fractures may not be easily identified and may also create an illusion of good effectiveness. The Monte Carlo method is used to calculate the porosity and permeability of multi-scale fractures, and there is a negative correlation between porosity and scale size. The order from large to small is micro-scale, small-scale, and large-scale. The magnitude of permeability at different scales shows an opposite pattern to porosity; that is, the larger the scale of the fracture, the greater the permeability. From the perspective of fracture connectivity, there is a positive correlation between fracture connectivity and fracture scale, with large-scale fractures having the best connectivity and micro-scale fractures having the worst connectivity. This difference is because the fracture scale, density, and orientation of different scale fractures are different, which affects the degree of fracture connectivity (Figure 8). This is consistent with Ortega et al. (2006) recognition that the impact of fracture scale effects on fracture parameters (fracture density, aperture) needs to be considered when calculating fracture parameters (Ortega et al., 2006).

Multiscale fractures are important storage spaces, and production practice has shown that natural fractures of different scales have significantly different effects on tight and low-permeability reservoirs and on oil and gas. Large scale fractures usually affect the preservation of oil and gas, while small and medium-sized fractures control the permeability system of tight reservoirs. Microscale fractures mainly play a storage role (Strijker et al., 2012; Lyu et al., 2019). Therefore, we compared the contribution rates of porosity and permeability in the multi-scale fracture system of the Qingshimao gas field, as well as the porosity and permeability in the matrix. Here, we established the relationship between multi-scale fracture porosity and permeability by analyzing the relevant parameters of matrix porosity and permeability, as well as the density distribution of multi-scale fractures (Figure 9). It can be seen that the contribution of matrix and fractures of different scales to the porosity and permeability of the reservoir is different. The contribution to porosity in descending order is matrix, micro-scale fractures, small-scale fractures, and large-scale fractures. The contribution rate of matrix porosity is 85%–95%, with an average of 88.6%; The contribution rate of micro-scale fracture

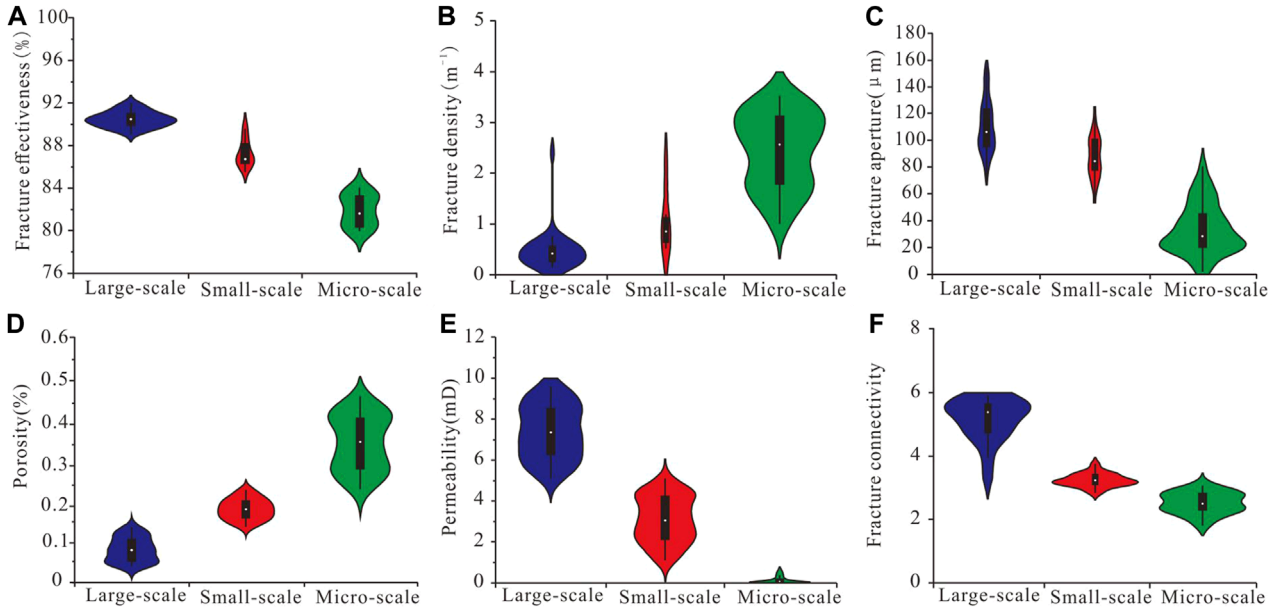

FIGURE 8
Distribution of fracture parameters at different scales. **(A)**Distribution of fracture effectiveness at different scales **(B)**Distribution of fracture density at different scales **(C)**Distribution of fracture aperture at different scales **(D)**Distribution of fracture porosity at different scales **(E)**Distribution of fracture permeability at different scales **(F)**Distribution of fracture connectivity at different scales.

porosity is 5%–11%, with an average of 7.4%; The contribution rate of small-scale fracture porosity is 0%–4%, with an average of 2.8%; The contribution rate of large-scale fracture porosity is 0%–2%, with an average of 1.2%. From the perspective of the contribution of permeability, its contribution in descending order is large-scale fractures, small-scale fractures, matrix, and micro-scale fractures. The contribution of permeability provided by the matrix is 5%–17%, with an average of 10%; Micro-scale fractures do not contribute significantly to reservoir permeability, averaging 3.2%, but they provide good porosity and can effectively communicate between intergranular and intragranular pores; The contribution of permeability of small-scale and large-scale fractures is 5–100 times that of matrix permeability. Small-scale fractures contribute 16%–43% to reservoir permeability, with an average of 24.4%. Due to the influence of layer control, they can provide important seepage channels and storage space for the tight sandstone reservoir in the Qingshimao gas field. Large-scale fractures have a significant contribution to reservoir permeability, mainly distributed in the range of 56%–70%, with an average of 62.4%. Due to the influence of throughgoing penetration, they have good connectivity and damage the reservoir, which can greatly improve the permeability and permeability of the reservoir (Figure 10).

Debenham et al. (2019) described and discussed the spatial distribution of porosity and permeability of microscale fractures in tight sandstone reservoirs and determined that micro-scale fracture changes can effectively improve reservoir permeability (Debenham et al., 2019). Hennings et al. (2012) determined through the analysis of the contribution of large-scale fractures to reservoirs and their control over reservoir performance that large-scale fractures can significantly improve reservoir properties and enhance reservoir performance (Hennings et al., 2012). Although

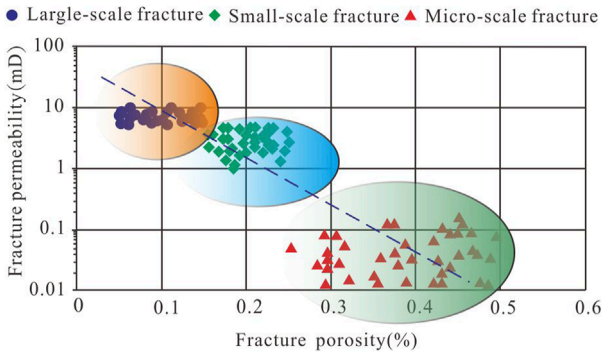

FIGURE 9
Relationship between fracture porosity and permeability.

they have made significant contributions to the study of the effect of fractures on reservoirs, there needs to be more research on the effect of multi-scale fractures on reservoirs. Therefore, we systematically evaluated and discussed the contribution and control of multi-scale fractures on reservoirs in the study area by considering the changes in the distribution patterns of different parameters of multi-scale fractures. We determined that different scale fractures have different control effects on the reservoir. Namely, micro-scale fractures can effectively communicate intergranular and intragranular pores, small-scale fractures can provide important seepage channels and reservoir space, and large-scale fractures can damage the reservoir. However, they can greatly improve the permeability and seepage capacity of the reservoir.

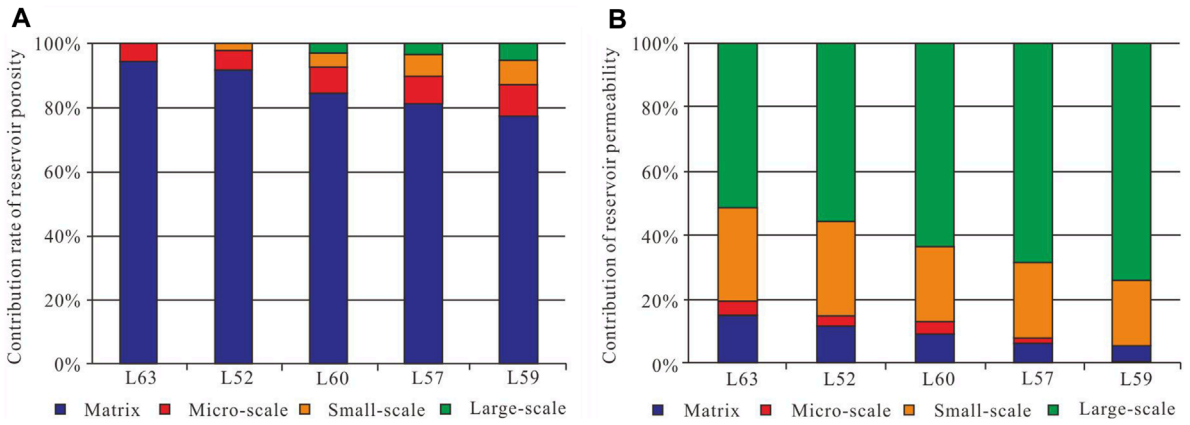

FIGURE 10
Shows the contribution rate of multi-scale fractures to the reservoir. **(A)** Multi-scale fracture porosity contribution rate. **(B)** Contribution of multi-scale fracture permeability.

5.2 The impact of multi-scale fracture development on the productivity of oil and gas wells

The porosity and permeability of tight sandstone reservoirs are relatively low, and fractures of different scales form a well-connected continuous network in space, which can serve as effective seepage channels and provide certain storage space for tight sandstone reservoirs. A well-connected network is a key factor for the formation of high-quality contiguous reservoirs and the achievement of high and stable production in tight sandstone reservoirs (Sanderson et al., 2018; Braathen et al., 2020; Lucca et al., 2020; Mercuri et al., 2020; Rabbel et al., 2021). Due to the different fracture sizes and connectivity of different scale configurations in different blocks of the Qingshimao area, the effectiveness and connectivity of fractures, as well as the contribution of fractures to reservoirs under different network structure modes are affected. Therefore, based on the quantitative characterization of multi-scale fractures in the tight sandstone reservoir in the Qingshimao area, we considered factors such as the fracture group and orientation, the size of the fracture scale, and the density of fractures. Based on the spatial combination patterns of fractures of different scales, we divided the study area into network structure patterns. Four types of seam network structures have been established: multi-scale fracture network with high density and multi multi-orientations, multi-scale fracture network with moderate-high density and dual orientations, small-scale fracture network with moderate density and dual orientations, small-scale fracture network with low density and single orientation (Figure 11).

The structural pattern of the first type of fracture network is located at the end and overlapping area of the fault. It has a multi-scale fracture network system with high fracture density, multiple orientations (mainly developing three to four fracture orientations), strong connectivity, and greatly improves the physical properties of the tight reservoir. It can form a large area of continuous, high-quality reservoirs. According to the distance relationship diagram between water and gas production and the fault (Figure 12), in this mode, the water production of a single well is high, and the gas production is low. This situation may be due to the large-scale fractures (throughgoing fractures and small faults) developed in this type of fracture network, which are prone to vertical connectivity, thereby damaging the integrity of the cap rock and causing natural gas leakage or upward layers-system adjustment. The fractures formed by it have played a destructive role in controlling storage and reservoirs.

The second type of fracture network structure pattern is located 0.5km–1.3 km near the fault, mainly developing two sets of fractures, with multi-scale throughgoing fractures as the main type. The degree of fracture development is high, and the connectivity is good, effectively improving the tight reservoir's physical properties and horizontal continuity. It can form a high-quality reservoir with regional continuity. The gas and water production relationship diagram shows that this mode has high gas and water production, making it the mode with the highest single well production and a favorable area for natural gas enrichment. This phenomenon may be because the fracture density is relatively high and the connectivity is relatively good in this mode, which can effectively improve the reservoir. However, it does not cause damage to the reservoir and is conducive to the enrichment of natural gas. The fractures formed in this mode are key in controlling reservoir and reservoir.

The third type of fracture network structure pattern is located within the range of 1.3–2.3 km from the fault. It mainly develops two sets of fractures, mainly small and medium-sized bed-confined fractures and partially throughgoing fractures. The fracture density and connectivity are moderate, which can obtain a certain production capacity. Fracturing is needed to improve the reservoir effectively. Its gas and water production are relatively low and cannot form a continuous high-quality reservoir. The fractures formed in this pattern play an adjusting role in controlling the reservoir.

The fourth type of fracture network structure mode is located in the parent rock area with high mud content > 2.3 km away from the fault. The orientation of the fractures is single, mainly consisting of small-scale bed-confined and micro-scale fractures. The fracture density is low, the connectivity is poor, and it cannot form a

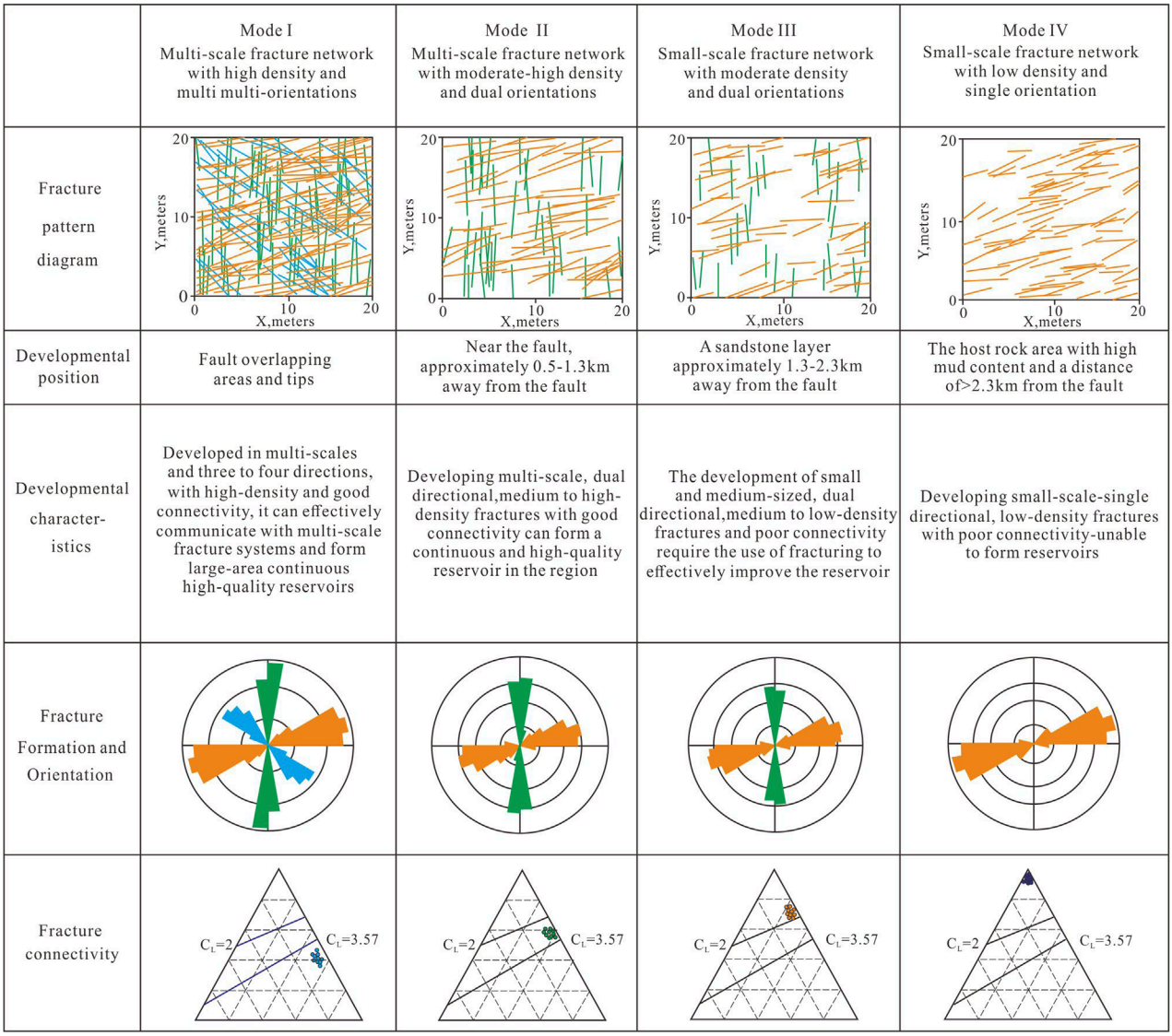

FIGURE 11
Structural pattern division of multi-scale fracture network.

reservoir. Its role in controlling the tight sandstone reservoir in the Qingshimao area is insignificant. Therefore, the Qingshimao area is greatly influenced by different fracture network structural patterns, and the differences between these patterns play an important role in the distribution of gas and water, which is one of the important reasons for the complexity of gas and water in the Qingshimao area.

Prabhakaran et al. (2021) studied the network structure pattern of reservoirs using large-scale fractures, emphasizing the inherent changes in the natural fracture network structure pattern. The results showed that the changes in the fracture network structure pattern cannot only consider the influence of a single factor (Prabhakaran et al., 2021). Ghosh and Mitra. (2009) considered the influence of fracture set and orientation, fracture density in their study of fracture connectivity and spatial configuration relationships. They concluded that multiple fracture systems and high density have a significant impact on connectivity (Ghosh and Mitra, 2009). Although scholars' research results have played an important role in fracture connectivity and network spatial structure patterns, there is still a lack of research on multi-scale and multi-factor aspects. Therefore, we propose a multi-scale fracture network structure pattern prediction method that considers multiple factors. By comprehensively discussing the spatial configuration relationship of multi-scale fractures in tight sandstone reservoirs, taking into account multiple factors such as fracture set and orientation, fracture scale, fracture density, fracture length, etc. and the control effect of fractures on the reservoir, we have determined the development patterns of fractures under different network structure patterns.

Understanding the spatial configuration relationship of fractures and their control over reservoirs can help determine the impact of fractures on reservoirs and the development of fractures under this network pattern. If one wants to understand the spatial configuration relationship of fractures and their control over

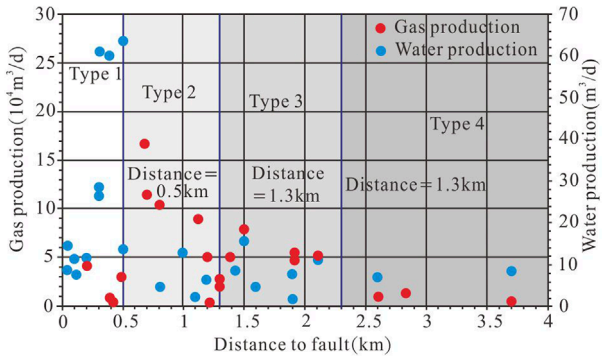

FIGURE 12
The relationship between gas production, water production, and distance from faults under four types of fracture network structure modes.

reservoirs, it is necessary to classify the scale of fractures and clarify the development characteristics of fractures at different scales rather than analyzing and discussing fractures at a single scale. When studying the spatial configuration relationship of fractures, it is necessary to consider multiple factors, including the fracture set and orientation of fractures, fracture scale, fracture density, fracture length, etc., rather than just considering the influence of one factor. This multi-scale and multi-factor consideration method helps to infer how fracture density, fracture connectivity, and fracture scale control reservoirs and helps to understand better and promote the development of multi-scale fracture network structure patterns in spatial configuration relationships.

6 Conclusion

1. A multi-scale fracture system is developed in the tight sandstone reservoir of the Qingshimao gas field in the Ordos Basin. The related parameters of micro, small, and large-scale fractures differ, but there are regular changes. Micro-scale fractures have high density, high porosity (0.1%–0.6%), and low permeability (0.01–0.1mD), it has the function of communicating matrix pores and reservoir space. Small-scale fractures are moderate compared to micro and large-scale fractures and are important flow channels for tight sandstone reservoirs in the study area. Large-scale fractures have a large length and aperture, good connectivity, and can provide important permeability (8-10mD) for tight reservoirs. However, the fracture density is relatively low, and the porosity provided for the reservoir is limited (0.07%–0.15%).
2. Based on the development characteristics of different types of fractures in the Qingshimao area, four types of fracture network structural models have been established. Different fracture network structures have different impacts on the production capacity of the Qingshimao gas field. Multi-scale fracture network with high density and multi-orientations can damage the integrity of the cover layer, causing natural gas leakage or adjustment to the upper layer system. Multi-scale fracture network with moderate-high density and dual orientations can effectively improve the physical properties and lateral continuity of tight reservoirs, making it a favorable area for natural gas enrichment. Small-scale fracture network with moderate density and dual orientations can achieve certain production capacity, but it requires the use of hydraulic fracturing to obtain commercial airflow. Small-scale fracture network with low density and single orientation cannot form a reservoir, and it has little effect on the control of tight sandstone reservoirs in the Qingshimao area.
3. The research results of this work are of great significance for future studies on the development characteristics and quantitative evaluation of multi-scale fractures. At the same time, they provide insights into the control and storage effects of multi-scale fractures and the development of multi-scale fracture network structural patterns in spatial configuration relationships. Increasing oil and gas development capacity has become crucial in the current context of energy transition. It is necessary to focus on this aspect of development not only in conventional oil and gas extraction, but also in the exploration and development of unconventional oil and gas and hydrocarbons.

Data availability statement

The raw data supporting the conclusions of this article will be made available by the authors, without undue reservation.

Author contributions

JeW: Conceptualization, Writing–original draft, Writing–review and editing. JpW: Conceptualization, Writing–original draft, Writing–review and editing. YZ: Data curation, Writing–review and editing. DZ: Formal Analysis, Writing–review and editing. LS: Data curation, Writing–review and editing. JL: Formal Analysis, Writing–review and editing. WW: Investigation, Writing–review and editing. LG: Methodology, Writing–review and editing. ZL: Writing–review and editing. SG: Writing–review and editing.

Funding

The author(s) declare that financial support was received for the research, authorship, and/or publication of this article. This research was funded by Research on Key Technologies for Improving Oil Recovery of Tight Sandstone Gas Reservoirs in China National Petroleum Corporation's Major Science and Technology Project (2023ZZ25); "Research on Reservoir Formation Characteristics, Main Control Factors, and Development Technology Countermeasures of Qingshimao Gas Field" Technology Project of Changqing Oilfield Company of China National Petroleum Corporation (2022D-JB04); National Natural Science Foundation of China (Grant No. 42172161), Natural Science Foundation of Heilongjiang Province (Grant No. YQ2021D006).

Conflict of interest

Authors JpW, YZ, DZ, LS, JL, and WW were employed by Exploration and Development Research Institute of China Petroleum Changqing Oilfield Company.

The remaining authors declare that the research was conducted in the absence of any commercial or financial relationships that could be construed as a potential conflict of interest.

The authors declare that this study received funding from China National Petroleum Corporation and Changqing Oilfield Company of China National Petroleum Corporation. The funder had the following involvement in the study: data collection and analysis.

Publisher's note

References

Aubert, I., Lamarche, J., and Léonide, P. (2021). Ternary fault permeability diagram: An innovative way to estimate fault zones hydraulics. *J. Struct. Geol.* 147, 104349. doi:10.1016/j.jsg.2021.104349

Bagni, F. L., Bezerra, F. H., Balsamo, F., Maia, R. P., and Dall'Aglio, M. (2020). Karst dissolution along fracture corridors in an anticline hinge, Jandaíra Formation, Brazil: implications for reservoir quality. *Mar. Petroleum Geol.* 115, 104249. doi:10.1016/j.marpetgeo.2020.104249

Balberg, I., Anderson, C. H., Alexander, S., and Wagner, N. (1984). Excluded volume and its relation to the onset of percolation. *Phys. Rev. B, Condens. matter* 30 (7), 3933–3943. doi:10.1103/PhysRevB.30.3933

Balberg, I., and Binenbaum, N. (1983). Computer study of the percolation threshold in a two-dimensional anisotropic system of conducting sticks. *Phys. Rev. B, Condens. matter* 28 (7), 3799–3812. doi:10.1103/PhysRevB.28.3799

Balsamo, F., La Bruna, V., Bezerra, F. H., Dall Aglio, M., Bagni, F. L., Silveira, L. G., et al. (2023). Mechanical stratigraphy controls fracture pattern and karst epigenic dissolution in folded Cretaceous carbonates in semiarid Brazil. *Mar. Petroleum Geol.* 155, 106409. doi:10.1016/j.marpetgeo.2023.106409

Berkowitz, B. (1995). Analysis of fracture network connectivity using percolation theory. *Math. Geol.* 27 (4), 467–483. doi:10.1007/BF02084422

Bertrand, L., Geraud, Y., Garzic, E. L., Place, J., Diraison, M., Walter, B., et al. (2015). A multiscale analysis of a fracture pattern in granite; a case study of the Tamariu Granite, Catalunya, Spain. *J. Struct. Geol.* 78, 52–66. doi:10.1016/j.jsg.2015.05.013

Birkholzer, J. T., Morris, J., Bargar, J. R., Brondolo, F., Cihan, A., Crandall, D., et al. (2021). A new modeling framework for multi-scale simulation of hydraulic fracturing and production from unconventional reservoirs. *Energies (Basel)* 14 (3), 641. doi:10.3390/en14030641

Braathen, A., Petrie, E., Nystuen, T., Sundal, A., Skurtveit, E., Zuchuat, V., et al. (2020). Interaction of deformation bands and fractures during progressive strain in monocline - san Rafael Swell, Central Utah, USA. *J. Struct. Geol.* 141 (104219), 104219. doi:10.1016/j.jsg.2020.104219

Cao, D. S., Zeng, L. B., Gomez-Rivas, E., Gong, L., Liu, G. P., Lu, G. Q., et al. (2024). Correction of linear fracture density and error analysis using underground borehole data. *J. Struct. Geol.* 105152, 105152. doi:10.1016/j.jsg.2024.105152

Casini, G., Hunt, D. W., Monsen, E., and Bounaim, A. (2016). Fracture characterization and modeling from virtual outcrops. *AAPG Bull.* 100 (01), 41–61. doi:10.1306/09141514228

Debenham, N., Farrell, N. J. C., Holford, S. P., King, R. C., and Healy, D. (2019). Spatial distribution of micrometre-scale porosity and permeability across the damage zone of a reverse-reactivated normal fault in a tight sandstone: insights from the Otway Basin, SE Australia. *Basin Res.* 31, 640–658. doi:10.1111/bre.12345

Farouk, S., Qteishat, A., Sen, S., Ahmad, F., El-Kahtany, K., Collier, R., et al. (2023). Characterization of the gas-bearing tight paleozoic sandstone reservoirs of the risha field, Jordan: inferences on reservoir quality and productivity. *Arabian J. Sci. Eng.* doi:10.1007/s13369-024-09000-x

Fernández-Ibáñez, F., DeGraff, J. M., and Ibrayev, F. (2018). Integrating borehole image logs with core: a method to enhance subsurface fracture characterization. *AAPG Bull.* 102 (06), 1067–1090. doi:10.1306/0726171609317002

Fu, J. H., Li, S. X., Guo, Q. H., Guo, W., Zhou, X. P., and Liu, J. Y. (2022a). Enrichment conditions and favorable area optimization of continental shale oil in Ordos Basin. *Acta Pet. Sin.* 43 (12), 1702–1716. doi:10.7623/syxb202212003

Fu, X. F., Gong, L., Su, X. C., Liu, B., Gao, S., Yang, J. G., et al. (2022b). Characteristics and controlling factors of natural fractures in continental tight-oil shale reservoir. *Miner. (Basel).* 12 (12), 1616. doi:10.3390/min12121616

Fu, X. F., Su, X. C., Gong, L., Wang, Q. Q., Gao, S., and Xie, Z. H. (2023). Control of faults and fractures on shale oil enrichment. *Geoenergy Sci. Eng.* 228, 212080. doi:10.1016/j.geoen.2023.212080

Gale, J. F. W., Laubach, S. E., Olson, J. E., Eichhubl, P., and Fall, A. (2014). Natural fractures in shale: a review and new observations. *AAPG Bull.* 98 (11), 2165–2216. doi:10.1306/08121413151

Gale, J. F. W., Reed, R. M., and Holder, J. (2007). Natural fractures in the Barnett Shale and their importance for hydraulic fracture treatments. *AAPG Bull.* 91 (4), 603–622. doi:10.1306/11010606061

German, M., Salim, A. H., Michael, R., Russell, F., Mohamed, B., and Carlos, T. V. (2023). Assessment of true formation resistivity and water saturation in deeply invaded tight-gas sandstones based on the combined numerical simulation of mud-filtrate invasion and resistivity logs. *Petrophysics.* 64 (4), 502–517. doi:10.30632/PJV64N4-2023a2

Ghanizadeh, A., Clarkson, C. R., Aquino, S., Ardakani, O. H., and Sanei, H. (2015). Petrophysical and geomechanical characteristics of Canadian tight oil and liquid-rich gas reservoirs: I. Pore network and permeability characterization. *Fuel Guildf.* 153 (2015), 664–681. doi:10.1016/j.fuel.2015.03.020

Ghosh, K., and Mitra, S. (2009). Two-dimensional simulation of controls of fracture parameters on fracture connectivity. *AAPG Bull.* 93 (11), 1517–1533. doi:10.1306/07270909041

Gong, L., Cheng, Y. Q., Gao, S., Gao, Z. Y., Feng, J. R., and Wang, H. T. (2023a). Fracture connectivity characterization and its controlling factors in the Lower Jurassic tight sandstone reservoirs of eastern Kuqa. *Earth Sci.* 48 (07), 2475–2488. doi:10.3799/dqkx.2022.066

Gong, L., Fu, X. F., Wang, Z. S., Gao, S., Jabbari, H., Yue, W. T., et al. (2019a). A new approach for characterization and prediction of natural fracture occurrence in tight oil sandstones with intense anisotropy. *AAPG Bull.* 103 (6), 1383–1400. doi:10.1306/12131818054

Gong, L., Liu, K., and Ju, W. (2023b). Editorial: advances in the study of natural fractures in deep and unconventional reservoirs. *Front. earth Sci. (Lausanne)* 2023, 10. doi:10.3389/feart.2022.1096643

Gong, L., Su, X. C., Gao, S., Fu, X. F., Jabbari, H., Wang, X. X., et al. (2019c). Characteristics and formation mechanism of natural fractures in the tight gas sandstones of Jiulongshan gas field, China. *J. Petroleum Sci. Eng.* 175, 1112–1121. doi:10.1016/j.petrol.2019.01.021

Gong, L., Wang, J., Gao, S., Fu, X. F., Liu, B., Miao, F. B., et al. (2021b). Characterization, controlling factors and evolution of fracture effectiveness in shale oil reservoirs. *J. Petroleum Sci. Eng.* 203, 108655. doi:10.1016/j.petrol.2021.108655

Guerriero, V., Iannace, A., Mazzoli, S., Parente, M., Vitale, S., and Giorgioni, M. (2010). Quantifying uncertainties in multi-scale studies of fractured reservoir analogues; implemented statistical analysis of scan line data from carbonate rocks. *J. Struct. Geol.* 32 (9), 1271–1278. doi:10.1016/j.jsg.2009.04.016

Guerriero, V., Vitale, S., Ciarcia, S., and Mazzoli, S. (2011). Improved statistical multi-scale analysis of fractured reservoir analogues. *TECTONOPHYSICS* 504 (1-4), 14–24. doi:10.1016/j.tecto.2011.01.003

Guo, Y. Q., Wang, M. X., Guo, B. C., Cai, Z. C., and Hui, L.(2020). Sedimentary system characteristics and paleographic evolution of upper paleozoic of northern west margin, Ordos Basin. *J. North. University (Nat. Sci. Edi.)* 50(01), 93–104. doi:10.16152/j.cnki.xdxbzr.2020-01-013

He, J. C., Yu, H. J., He, G. H., Zhang, J., and Li, Y. (2021). Natural gas development prospect in Changqing gas province of the Ordos Basin. *Nat. Gas. Ind.* 41 (08), 23–33. doi:10.3787/j.issn.1000-0976.2021.08.003

Hennings, P., Allwardt, P., Paul, P., Zahm, C., Reid, R., Jr., Alley, H., et al. (2012). Relationship between fractures, fault zones, stress, and reservoir productivity in the Suban gas field, Sumatra, Indonesia. *AAPG Bull.* 96 (4), 753–772. doi:10.1306/08161109084

Jia, C. Z., Zheng, M., and Zhang, Y. F. (2012). Unconventional hydrocarbon resources in China and the prospect of exploration and development. *Petroleum Explor. Dev.* 39 (02), 139–146. doi:10.1016/S1876-3804(12)60026-3

Jiang, F. J., Jia, C. Z., Pang, X. Q., Jiang, L., and Zhang, C. L. (2023). Upper paleozoic total petroleum system and geological model of natural gas enrichment in Ordos Basin, NW China. *Petroleum exploration and development* 50 (02), 250–261. doi:10.11698/PED.20220602

Laubach, S. E., Lamarche, J., Gauthier, B. D. M., Dunne, W. M., and Sanderson, D. J. (2018). Spatial arrangement of faults and opening -mode fractures. *J. Struct. Geol.* 108, 2–15. doi:10.1016/j.jsg.2017.08.008

Loza Espejel, R., Alves, T. M., and Blenkinsop, T. G. (2020). Multi-scale fracture network characterisation on carbonate platforms. *J. Struct. Geol.* 140 (104160), 104160. doi:10.1016/j.jsg.2020.104160

Lucca, A., Storti, F., and Molli, G. (2020). Extensional fracture network attribute distribution in faulted thick sandstone strata: compione Fault, Northern Apennines, Italy. *J. Struct. Geol.* 131 (103954), 103954. doi:10.1016/j.jsg.2019.103954

Lyu, W., Zeng, L., Zhou, S., Du, X., Xia, D., Liu, G., et al. (2019). Natural fractures in tight-oil sandstones: a case study of the upper triassic Yanchang formation in the southwestern Ordos Basin, China. *AAPG Bull.* 103 (10), 2343–2367. doi:10.1306/0130191608617115

Manzocchi, T. (2002). The connectivity of two-dimensional networks of spatially correlated fractures. *Water Resour. Res.* 38 (9), 1162. doi:10.1029/2000WR000180

Mercuri, M., Carminati, E., Tartarello, M. C., Brandano, M., Mazzanti, P., Brunetti, A., et al. (2020). Lithological and structural control on fracture frequency distribution within a carbonate-hosted relay ramp. *J. Struct. Geol.* 137, 104085. doi:10.1016/j.jsg.2020.104085

Micheal, M., Xu, W., Xu, H., Zhang, J., Jin, H., Yu, H., et al. (2021). Multi-scale modelling of gas transport and production evaluation in shale reservoir considering crisscrossing fractures. *J. Nat. gas Sci. Eng.* 95 (104156), 104156. doi:10.1016/j.jngse.2021.104156

Nixon, C. W., Sanderson, D. J., and Bull, J. M. (2012). Analysis of a strike-slip fault network using high resolution multibeam bathymetry, offshore NW Devon U.K. *Tectonophysics* 541-543, 69–80. doi:10.1016/j.tecto.2012.03.021

Nwabia, F. N., and Leung, J. Y. (2021). Probabilistic history matching of multi-scale fractured reservoirs: Integration of a novel localization scheme based on rate transient analysis. *J. Nat. Gas Sci. Eng.* 94, 104067. doi:10.1016/j.jngse.2021.104067

Ortega, O. J., Marrett, R. A., and Laubach, S. E. (2006). A scale-independent approach to fracture intensity and average spacing measurement. *AAPG Bull.* 90 (2), 193–208. doi:10.1306/08250505059

Petrik, A., Vahle, C., Gianotten, I. P., Trøan, L. L., Rojo, L., and Galbraith, K. (2023). Quantitative characterisation of fracture connectivity from high-resolution borehole image logs. *Mar. petroleum Geol.* 155, 106405. doi:10.1016/j.marpetgeo.2023.106405

Prabhakaran, R., Urai, J. L., Bertotti, G., Weismuller, C., and Smeulders, D. M. J. (2021). Large-scale natural fracture network patterns: insights from automated mapping in the Lilstock (Bristol Channel) limestone outcrops. *J. Struct. Geol.* 150 (104405), 104405. doi:10.1016/j.jsg.2021.104405

Rabbel, O., Palma, O., Mair, K., Galland, O., Spacapan, J. B., and Senger, K. (2021). Fracture networks in shale-hosted igneous intrusions: processes, distribution and implications for igneous petroleum systems. *J. Struct. Geol.* 150 (104403), 104403. doi:10.1016/j.jsg.2021.104403

Sanderson, D. J., and Nixon, C. W. (2015). The use of topology in fracture network characterization. *J. Struct. Geol.* 72, 55–66. doi:10.1016/j.jsg.2015.01.005

Sanderson, D. J., Peacock, D. C. P., Nixon, C. W., and Rotevatn, A. (2018). Graph theory and the analysis of fracture networks. *J. Struct. Geol.* 125, 155–165. doi:10.1016/j.jsg.2018.04.011

Strijker, G., Bertotti, G., and Luthi, S. M. (2012). Multi-scale fracture network analysis from an outcrop analogue: a case study from the Cambro-Ordovician clastic succession in Petra, Jordan. *Mar. Petroleum Geol.* 38 (1), 104–116. doi:10.1016/j.marpetgeo.2012.07.003

Su, X. C., Gong, L., Fu, X. F., Gao, S., Zhou, X. P., and Lu, Q. (2023). Fracture distribution characteristics and effectiveness evaluation of tight sandstone reservoir of chang 7 member in Sanbian area, Ordos Basin. *Earth Sci.* 48 (07), 2601–2613. doi:10.3799/dqkx.2022.116

Sweeney, M. R., Hyman, J. D., Malley, D. O. ', Santos, J. E., Carey, J. W., and Stauffer, P. H. (2023). Characterizing the impacts of multi-scale heterogeneity on solute transport in fracture networks. *Geophys. Res. Lett.* 21 (50), 1–26. doi:10.1029/2023GL104958

Vasquez Serrano, A., Sampayo Rodriguez, M. F., Fitz Diaz, E., and Tolson, G. (2024). Kinematics, intensity, and spatial arrangement of extensional fractures in the Tuxtla-Malpaso fault system: Chiapas strike-slip fault province, southern Mexico. *J. Struct. Geol.* 180, 105062. doi:10.1016/j.jsg.2024.105062

Wang, J., Hu, C. G., Pan, Y. L., Huang, Q. J., Yuan, H. Q., and Gong, L. (2022). Fracture development characteristics and comprehensive evaluation of buried hill metamorphic reservoir in Jihua 1 area. *Chin. J. Geol.* 57 (02), 463–477. doi:10.12017/dzkx.2022.027

Watkins, H., Bond, C. E., Healy, D., and Butler, R. W. H. (2015). Appraisal of fracture sampling methods and a new workflow to characterise heterogeneous fracture networks at outcrop. *J. Struct. Geol.* 72, 67–82. doi:10.1016/j.jsg.2015.02.001

Watkins, H., Healy, D., Bond, C. E., and Butler, R. W. H. (2018). Implications of heterogeneous fracture distribution on reservoir quality; an analogue from the Torridon Group sandstone, Moine Thrust Belt, NW Scotland. *J. Struct. Geol.* 108, 180–197. doi:10.1016/j.jsg.2017.06.002

Yin, S., Sun, X. G., Wu, Z. H., Wang, Y. B., Zhao, J. Z., and Sun, W. H. (2022). Coupling control of tectonic evolution and fractures on the Upper Paleozoic gas reservoirs in the northeastern margin of the Ordos Basin. *J. Central South Univ. Sci. Technol.* 53 (09), 3724–3737. doi:10.11817/j.issn.1672-7207.2022.09.033

Zeng, L.B.(2010). Microfracturing in the upper triassic sichuan basin tight gas sandstones: tectonic, overpressure, and diagenetic origins. *AAPG Bull.* 94(12), 1811–1825. doi:10.1306/06301009191

Zeng, L. B., Gong, L., Guan, C., Zhang, B. J., Wang, Q. Q., Zeng, Q., et al. (2022). Natural fractures and their contribution to tight gas conglomerate reservoirs: a case study in the northwestern Sichuan Basin, China. *J. petroleum Sci. Eng.* 210, 110028. doi:10.1016/j.petrol.2021.110028

Zeng, L. B., Gong, L., Su, X. C., and Mao, Z. (2024). Natural fractures in deep to ultra-deep tight reservoirs:Distribution and development. *Oil Gas Geol.* 45 (01), 1–14. doi:10.11743/ogg20240101

Zeng, L. B., Gong, L., Zhang, Y. Z., Dong, S. Q., and Lyu, W. Y. (2023). A review of the genesis, evolution, and prediction of natural fractures in deep tight sandstones of China. *AAPG Bull.* 107 (10), 1687–1721. doi:10.1306/07052322120